Frostbyte:
Multi-Phase Lower Digital Freezing

BEE 4530: Computer-Aided Engineering: Applications to Biological Processes©

Team members: Benjamin Cooke, John Jaicks, Cameron Kitzinger, TJ Sheppard

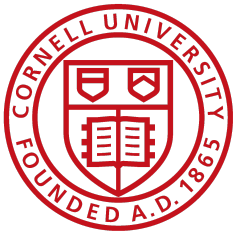

14 May 2021

TABLE OF CONTENTS

1.0 Executive Summary

Though frostbite is an affliction that has been commonly known for hundreds of years, its direct effect and dynamics have rarely been studied. With modern technology and an understanding of the human body, tissue freezing can now be modeled to fully understand its progression and once and for all resolve its procession. Here we used a high definition, multilayered, anatomically accurate 3D model of a foot subjected to a subfreezing environment to develop a novel understanding of the crucial parameters in frostbite prevention. The results, as shown in the form of cross-sectional temperature profile images, tell us that the toes freeze within the two-hour runtime where the middle of the foot does not. With little research before this, we believe that this model will be of great use to the scientific community and will likely lead to real solutions to come.

Keywords: Frostbite, Foot, Insulation, Transient Heat Flow, Freezing, Convective Heat Transfer, Multilayer

2.0 Introduction

2.1 Introduction

In freezing temperatures, chilblains, frostbite, and hypothermia become dangerous conditions that can lead to loss of appendage or death. Every year, over 1,000 people die from exposure to the cold, and far more experience symptoms that can range from painful frozen patches to widespread permanent tissue damage.[8] Although not generally life-threatening, the plight of frostbite and chilblains are a constant threat to anyone who frequents the outdoors. And while there is some research on related issues, no current studies that exist have managed to provide concrete scientifically based guidelines for the prevention of cold-induced damage.

Previous research has yielded several studies on the dynamics of heat loss from appendages[1][2][8][16][19], however, none specifically observe the effects on the foot, and certainly none with a detailed 3D model[1][3]. The difficult part about modeling a human foot comes from its complex shape and variable conditions involved with an insulative shoe and sock. The majority of currently available research is clinically based and focused more on frostbite remediation than prevention. The hoi polloi's understanding of how best to prevent damage from frostbite is based upon anecdotal evidence or personal experience. This project hopes to better understand how below-freezing temperatures lead to frostbite and permanent tissue damage and provides a useful model for future research. This will allow us and other researchers to begin to understand the effect of below-freezing temperatures that can be so consequential for so many people every year.

2.2 Problem Statement

Few frostbite experimental procedures can be conducted safely and ethically, but it is a phenomenon that needs to be studied to help reduce the incidence and severity of cases. Currently, there are no accurate foot models publicly available that can be used for testing environmental and physical conditions. Because of this, there is not a complete understanding of the factors involved in frostbite. We approached this lack of understanding by constructing an anatomically accurate 3D model of the foot including various relevant biological features[17]. We imported the model into COMSOL and implemented relevant material properties and governing equations. This results in bio-accurate geometry with realistic material properties that can serve as a basis for analysis under extreme cold environmental conditions. From this starting model, we are able to iterate rapidly different insulating regimes and establish clear and scientifically founded advice for preventing frostbite.

2.3 Design Objectives

The objective of this project is to model an insulated foot in below-freezing outer temperatures. To achieve this goal, we accomplished three main objectives.

1. Create an anatomically accurate foot model
    - Validate the aforementioned foot model
2. Test model under specific environmental and physical conditions
    - External heat transfer coefficient, thermal conductivity of insulating layers, metabolic generation, and specific heat capacity of biological tissues
3. Develop a fundamental understanding of important parameters for frostbite prevention
    - Provide guidelines for the amount or type of insulation at a specific temperature

3.0 Methods

3.1 Geometric Mesh Preparation

We created the geometric meshes for all layers of the foot in Autodesk Meshmixer using an stl file downloaded from the 3D model repository Thingiverse[17] shown in figure 1b. From this model, we applied a series of operations to create the various domains based on accumulated geometric parameters from previous scientific literature[5][6]. Figure 1a shows the mesh layers called “flesh,” “fat,” “inner sock,” “outer sock,” and “boot”, representing the outermost surface

mesh of these layers. The “skin” domain, however, refers to the space between the outer surface boundary of the skin and the inner surface boundary of the inner sock.

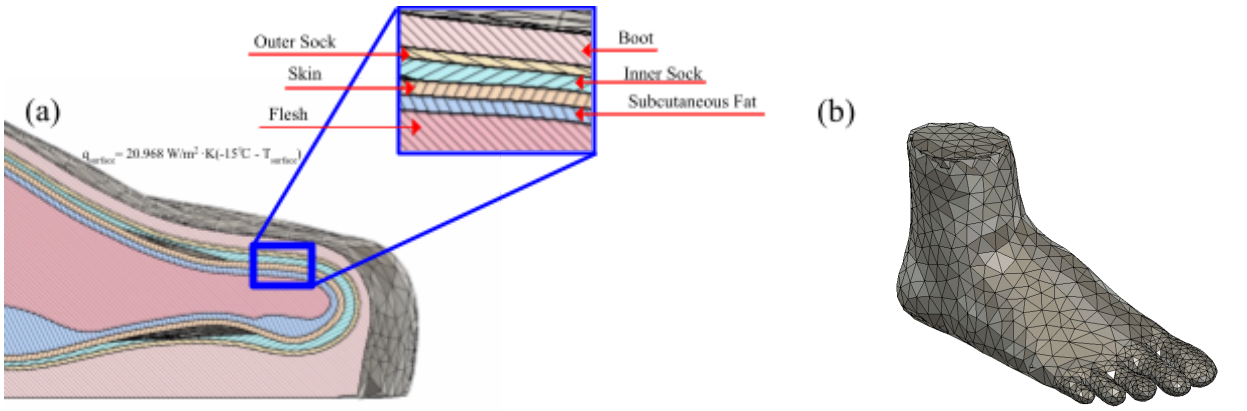

Fig. 1. (a) A planar cross section of the anatomical mesh foot model. We set variable layer thicknesses according to available literature. Note the larger subcutaneous fat pads on foot pressure points (in blue) which provide significant thermal insulation. (b) Shows the outer geometry of the biological domains for reference.

The downloaded file contained a surface mesh for a human leg. After cutting this mesh down to only include geometry below the ankle, we applied a universal scaling operation. This allowed us to set the overall length of the foot (measured from the tip of the pointer toe to the heel) to be representative of the average male foot size. In the final step of the preprocessing/cleaning procedure, we used a smoothing and flat fill tool to remove and re-mesh details concerning the toenails as these were unlikely to have any thermodynamic implications and greatly increased the complexity of the model in that region.

Once the beginning “skin” layer mesh (again, this nomenclature refers to the *outer* surface mesh of the solid skin layer) had been created the layer formation and inspection could begin. Using the “skin layer” as a starting point, we constructed the inner layers by isolating layers created from a hollowing operation on the original mesh. This allowed us to generate layers of designated thickness for the “skin,” “fat,” and “flesh” domains. Outer layers were created by first smoothing the toe region until it visually resembled a sock and then normally extruding from the existing faces by the desired thickness. The boot layer was created similarly to the sock layers but with an additional downward extrusion from the bottom of the expanded outer sock layer to create the outsole of the boot. The flesh layer was only dimensioned implicitly as it represents the innermost layer, i.e. the remaining volume once all other outer domains had been established. bone geometry was not included at this time primarily due to the lack of available matching models.

We achieved variable layer thickness for both fat and skin layers by setting the thickness of the layer to the average of the top and bottom thickness layers and then translating the layer upward by half of the absolute difference in thickness. This method was used to create different thicknesses on the top and bottom of the "fat" and "skin" domains. Visual contours were automatically generated on the bottom of the mesh that formed a topographic map of the bottom of the foot. To include the increased thickness of the subcutaneous fat layer around contact points with the ground, we selected the lowest areas using the topographic map of the foot and extruded out to a depth corresponding with researched values.

Once all of the high-density geometric meshes had been created we loaded them into Autodesk's Fusion 360 for dimensional analysis and visualization. Once we confirmed that the high-density mesh was accurate to the intended values the files were once again loaded into Meshmixer where the many manifold repairs, smoothing, and mesh reduction operations were applied until the mesh was brought to a point where it could be worked within COMSOL.

3.2 Governing Equations

Starting from the full heat transfer equation, we remove the convection terms for the sake of simplicity in our model. We decided that having a more accurate geometry is more important initially than hyper-realistic physics. The heat transfer equation is solved for transient temperature because that will be our main point of analysis. In this, we also include apparent specific heat, C_{pA} as we are dealing with subzero temperature changes and thus changing specific heat capacity as our layers freeze. Our resulting equation is shown below:

$$\frac{\partial T}{\partial t} = \frac{k}{\rho c_{pa}} \frac{\partial^2 T}{\partial x^2} + Q \qquad (1)$$

The changing specific heat was implemented as a range of values based on the known specific heat change in a wart around water freezing temperatures. We do this because the latent heat of freezing required for water in the tissue will change the specific heat around water freezing temperatures. This was done in COMSOL with a linear interpolation with values from temperatures ranging from T = -255℃ to T = 60℃. The values are detailed in Table 2 (Appendix 1).

The heat generation term "Q" included two different sources of heat in its current implementation. It had a general cellular metabolic generation ($q_{cellular}$) as listed in the relevant data section, as well as a bioheat contribution as shown below. Volumetric blood flow and metabolic generation were considered under the unique Qs term for each layer, as shown below:

$$Q = q_{cellular} + \rho_{blood} C_{p,blood} V_{blood} (T_{blood} - T) \qquad (2)$$

The aforementioned Bioheat equation, as described with the utilization of unique volumetric flow and cellular metabolic heat terms is presented below.

$$\text{Bioheat equation:} \frac{\partial T}{\partial t} = \frac{k}{\rho c_{pa}} \frac{\partial^2 T}{\partial x^2} + q_{cellular} + \frac{\rho_{bl} w_{bl} c_{bl}}{\rho c_{pa}} (T_{bl,a} - T) \quad (3)$$

Values for specific heat, density, and temperature of arterial blood were all taken from Holland et al[18]. Volumetric blood flow rate per volume tissue was taken from a study by J. Grayson which provided the values for right-hand anatomy[19]. It is believed this is a reasonable estimate due to the similarity of vasculature in distal appendages. The final implemented equation is presented below, including apparent specific heat and a combined heat generation term.

$$\text{Implemented equation:} \frac{\partial T}{\partial t} = \frac{k}{\rho c_{pa}} \frac{\partial^2 T}{\partial x^2} + Q \quad (4)$$

3.3 Boundary Conditions

In our model, we are implementing a convective flux boundary over the surface of the model. The outside temperature and windchill is the near most crucial facet of this simulation, and setting a reasonable constant would help us manage sub-zero scenarios. We are using this at both the top and bottom of the boot, as well as on all sides. To get our heat transfer coefficient in this implementation, we utilized the equation for forced convection over a flat surface, assuming that wind will always be traveling in a path parallel to the foot across its length. We utilized a wind speed of 15 mph, a characteristic length of 0.25 m (an average between open area length on the top and bottom of the foot), and thermal conductivity (0.025 W/mK), density (1.3082 kg/m^3), viscosity (1.7x10^{-5} kg/ms), and Prandtl number (.684) from the air at -15℃. Assuming it to be a reasonable average wind velocity for a cold day. We are assuming this to be our only boundary condition at the current time, as it applies in all directions for a large-scale model under windy conditions. The environmental temperature of -15℃ was implemented because it is not uncommon to reach this temperature during a cold winter day in Ithaca, NY.

$$h = \frac{k}{L} 0.664 \left(\frac{u_{inf} \rho L}{\mu}\right)^{1/2} Pr^{1/2} \quad (5)$$

$$q_{surface} = 20.968 \frac{W}{m^2 * K} (-15℃ - T_{surface}) \quad (6)$$

3.4 Initial Condition

Under our model, we assume that at time zero the entire geometry is at body temperature. This is a reasonable condition given the functionality of the body in ideal conditions. The thermal capacity of all non-biological domains does not appear significant in our analysis and therefore is given the same initial starting temperature as biological tissue.

$$T_{all}|_{t=0} = 36.85℃ \quad (7)$$

3.5 Relevant Data

The following two tables contain all of the necessary data that was entered into COMSOL to achieve our results. Table 1 (Appendix A) includes material property data and heat generation rates (where applicable) for all material domains. Table 2 (Appendix A) is representative of the interpolation function we used to model the freezing process. Note the huge increase in specific heat around -3℃ to account for the latent heat of freezing.

4.0 Results & Discussion

4.1 Graphical Results

The results of primary interest to us come in the form of cross-sectional temperature gradient views of the foot after the 120-minute test duration. One such view is provided around the toes (Figure 2) and another directly in the geometrical center of the foot (Figure 3).

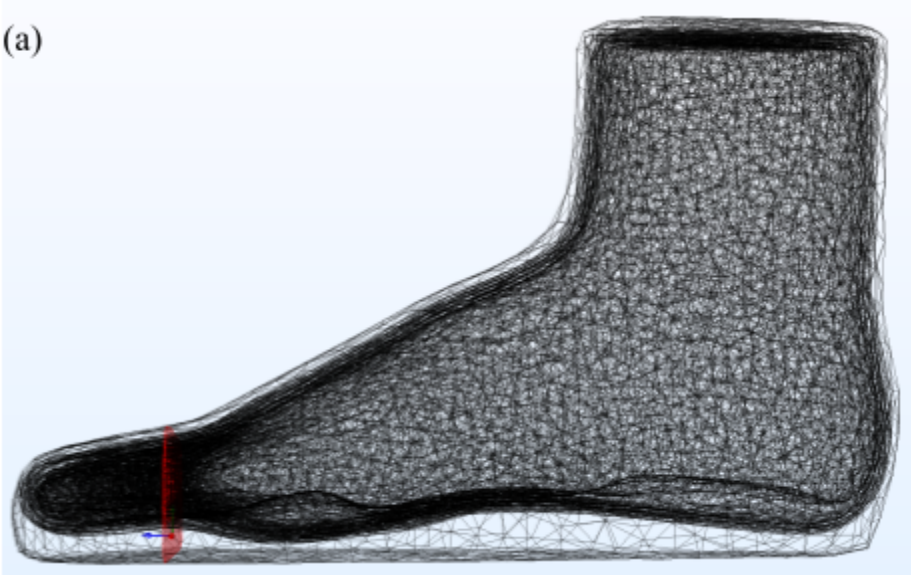

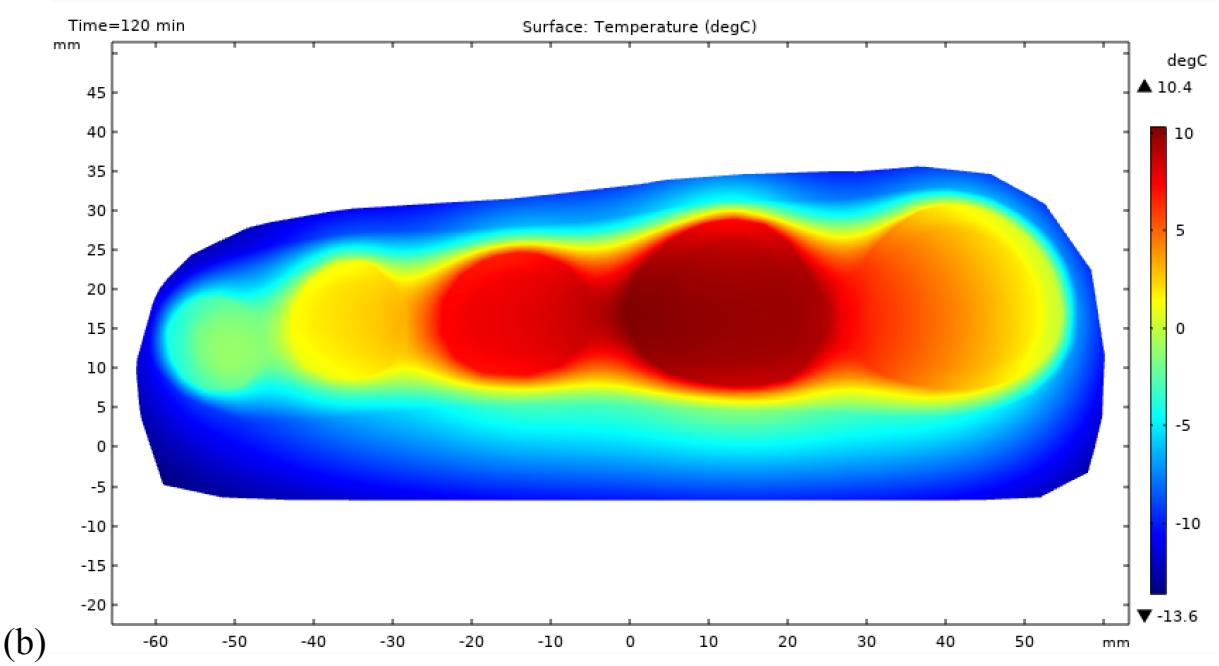

(b)

Fig. 2. (a) Profile of a cross section -107mm from the geometric origin of the foot model. (b) Pictured are the toe models after 2 hours exposed to an external temperature of -25C. We can see here that significant portions of the smaller and more exposed digits have been frozen resulting in significant tissue damage.

From the cross-section shown in Figure 2a, we see in Figure 2b that areas on the outskirts of the foot deal with the worst effects of the cold. Notably, the pinky toe (far left) appears to be entirely below 0℃, and the ring toe just beyond it is nearing the same range. This dictates serious freezing and detrimental levels of frostbite.

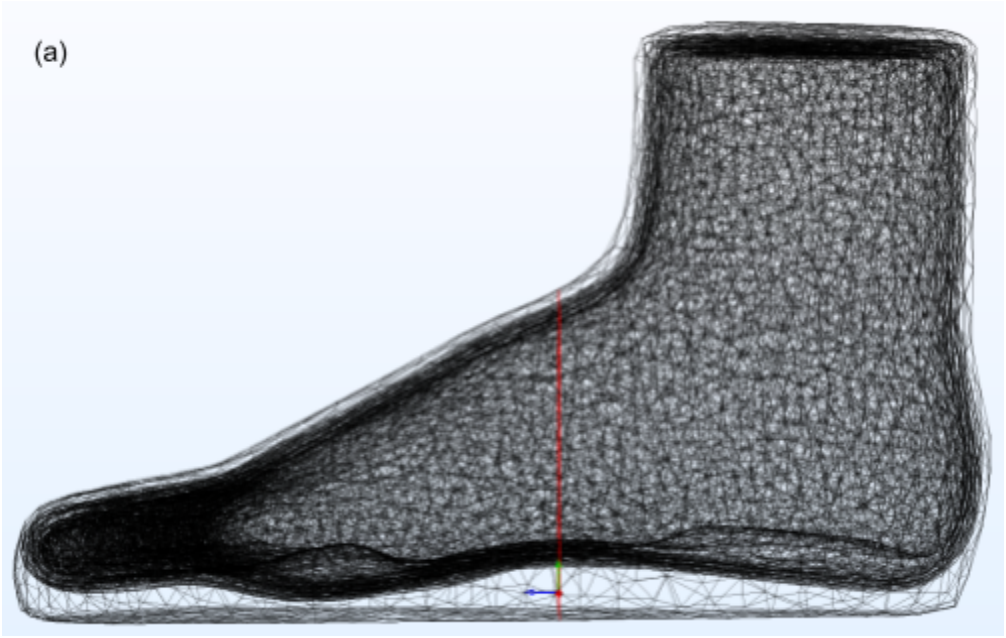

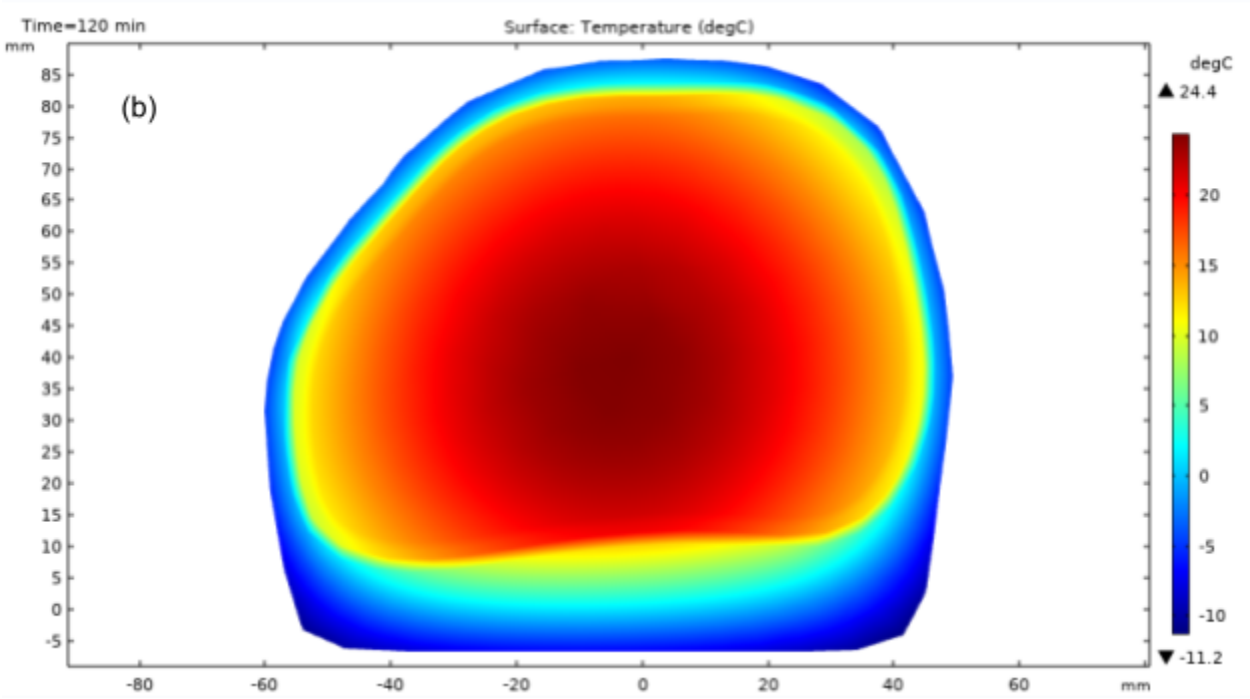

Fig. 3. (a) Profile of a cross section at the geometric origin of the foot model. (b) Pictured are the toe models after 2 hours exposed to an external temperature of 258K. Much of the foot tissue remains unfrozen but significantly chilled.

From the cross-section at the location in Figure 3a, Figure 3b shows that the center of the foot remains largely unharmed by the extreme weather but the skin does appear to be feeling the effects at a very steep gradient to the external.

In addition to the cross-sectional images that show us the actual temperature of specific sections, we were also interested in how much tissue froze, and where the depth of freezing could be approximated to, which is shown as a yellow boundary between blue and red regions (Figure 4). In the toe region, all tissue to the right of the yellow boundaries is at or below a temperature of 0℃. This displays as a rigid cutoff, but in reality, there will be a semi-frozen “mush” zone separating completely frozen tissue from completely unfrozen tissue.

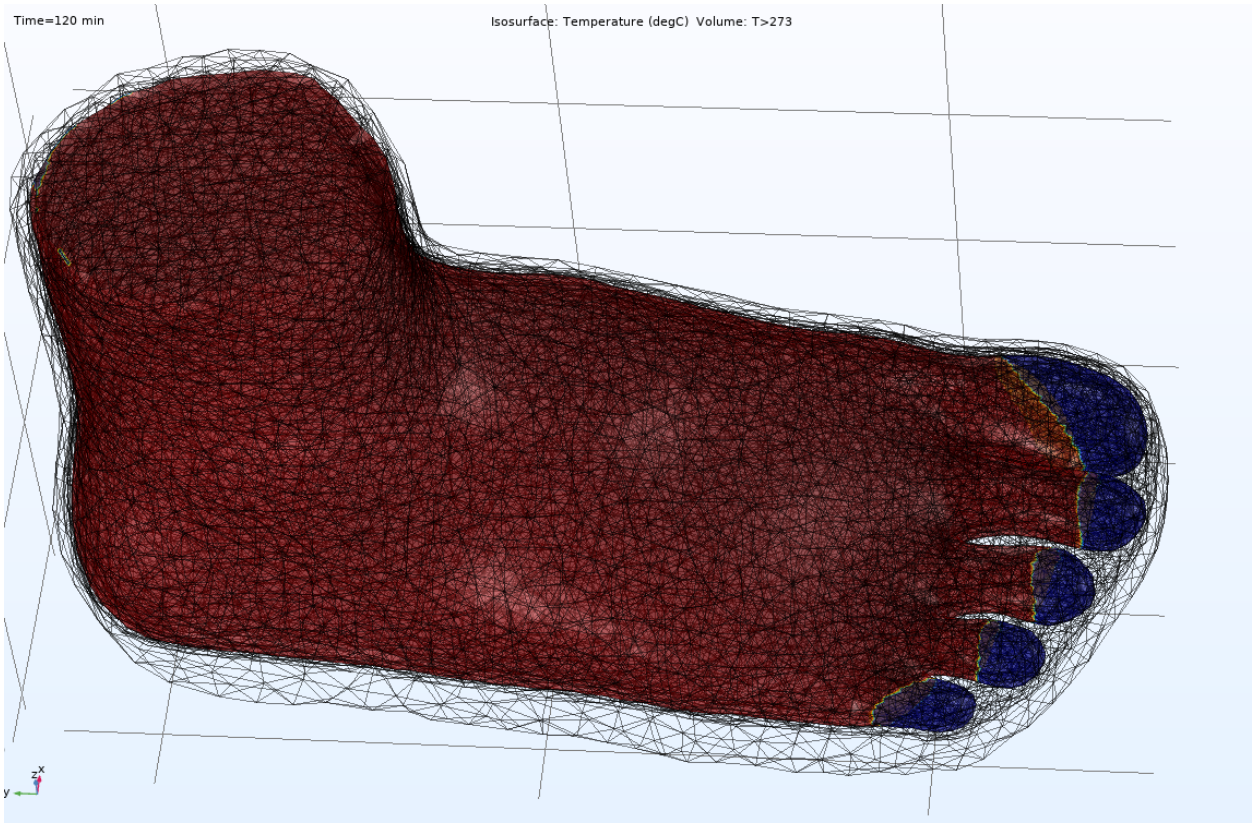

Fig. 4. 3D Isothermal contour shows progression of frozen front into biological tissue. Only the distal regions of the toes have frozen at the final 2 hour time. Note that while this figure depicts the freezing front as a crisp surface it is likely to occur in reality as a gradient transition, without a clear defined line between frozen and unfrozen tissue.

In Figure 4 we can see the distinct gradient point where tissue resides at our designated freezing point, 0℃. We see that the digits are the primary affected area of the conditions, progressing through the region as it approaches the central region of the foot.

The results of our simulation appear to show much of the digit anatomy has frozen. This is a slightly more hopeful picture than was cast by our previous attempts. The incorporation of a spike in specific heat to accommodate for the latent heat of freezing has significantly slowed the progression of the freezing front. Figures 2 and 3 show cross-sections across different regions of the geometry. Figure 2 in particular shows the extent of frostbite damage to the extremities of the foot. Much of the tissue in the smaller or more exposed toes is frozen, while the inner toes remain functional but significantly cooled. Figure 3 casts a far more hopeful picture as nearly all of the biological domain is still above 0°C (visualization of this is understandably difficult but the thickness of frozen tissue does not protrude more than the thickness of insulation). Figure 4 depicts in yellow the front at which freezing is progressing through the foot. All regions to the right of the barrier are frozen at this time. The freezing front has progressed a significant way

into the toes but the bulk of the biological domain remains unfrozen. This stacks up quite well against the experience of the authors given the external conditions established in our formulation.

4.2 Mesh Convergence

Mesh Convergence analysis ensured that our simulation reduced discretization error as much as possible. Variable mesh densities were made using the COMSOL built-in mesh densities (Extra Coarse, Coarser, Coarse, Normal, Fine, Finer). These settings created meshes with a variable number of elements. To achieve mesh convergence, we seek to minimize the change in a parameter per additional mesh element. The goal of this step is to gain confidence in the model. If the mesh is too coarse, the temperature values may not accurately reflect the process we hope to study, but if the mesh is too fine, it will take up more computational resources than necessary with little to no improvement in model accuracy. The temperature at each of the five points was recorded at the end of 120 minutes under the conditions previously described (Figure 5).

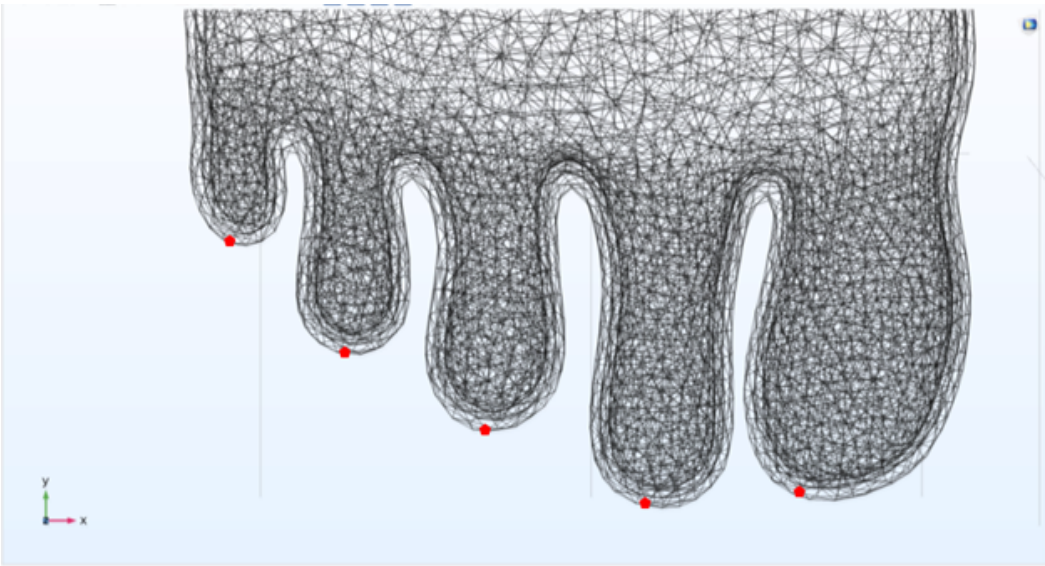

Fig. 5. Diagram showing the points used for mesh convergence. The coordinates of each point from the origin of the geometry are Big Toe (31, -149, 12), Pointer Toe (8, -151, 13.634), Middle Toe (-16, -140, 13), Fourth Toe (-36, -129, 11), Pinky Toe (-54, -112, 12)

Above shows the node points for each toe as calculated for in the mesh convergence. They are located at the tip of each toe to show that our most sensitive area contains as little discretization error as possible. For this geometry, convergence starts at the “Fine” setting, resulting in 991,651

nodes (Figure 6).

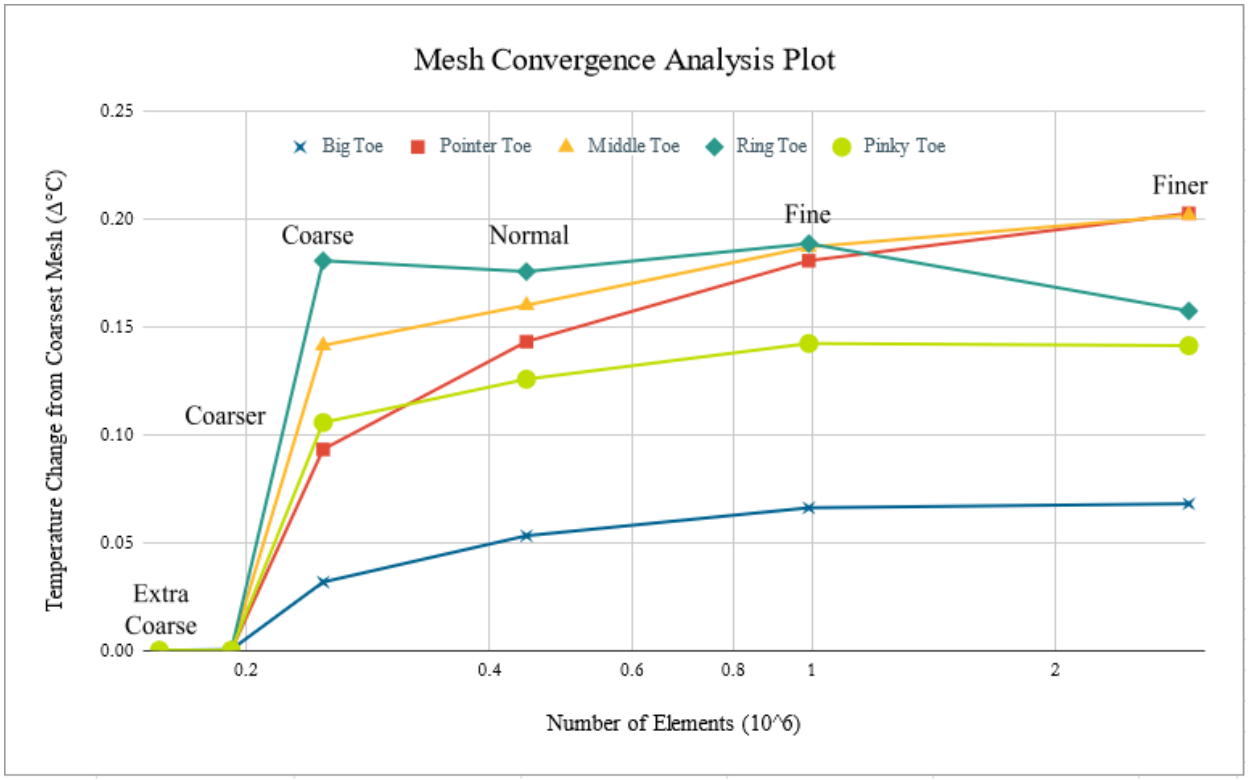

Fig. 6. Convergence plot showing temperature data from all five points as a relative change from the coarsest mesh. The change in temperature between one million and two million nodes is insignificant compared to the change in temperature between the other points, so we can conclude that the "Fine" mesh setting is sufficient. The settings used and element number are as follows: Extra Coarse (156,185), Coarser (191,666), Coarse (248,939), Normal (443,979), Fine (991,651), Finer (2,924,404). Note that the horizontal axis is a logarithmic scale. This is done to show the difference in the settings with lower mesh counts because the mesh settings are themself logarithmic in nature

The leveling off of the final temperature between the "Fine" and "Finer" mesh settings is how we know that we are not introducing novel discretization errors while still ensuring we are not needlessly using additional computational resources.

4.3 Sources of Error

After confirming that the mesh was dense enough for an accurate study from mesh convergence, we can reasonably claim that it is not introducing novel error. Further investigation into the sock and boot material properties is desired, particularly as we plan on investigating the best insulative regime to protect the foot against such damage. This model also includes very minimal cooling impact upon metabolic heat generation and blood flow. Current heat generation data includes the additional generation that would occur due to blood flow from the bioheat equations. Parameterizing the heat generation of specific domains in addition to apparent specific heat would greatly improve results. Additionally, we currently use one specific heat function for

all of the layers of flesh, which we hope to modify when more data or calculations are performed for each layer. This would not only make the model more biologically accurate but also help us refine our material properties. The modeling of blood flow will also be critical in establishing the effect of vasoconstriction, an important aspect of how and why extreme cold weather can cause severe tissue damage, at a later deadline.

4.4 Conclusion

These results give us a very reasonable starting point to begin conducting sensitivity analysis in which the real value of the model can be extracted. The level of tissue damage in this initial setup is ultimately not of interest as it is only representative of these exact conditions which may not be experimentally replicable in the real world. The systematic variation of significant parameters will help us begin to develop concrete (rather than anecdotal) guidance on how to best prevent damage as seen above.

5.0 Model Validation

5.1 Common Sense Validation

As we see in Figure 2, the temperature of the foot after two hours sees freezing on the surface, and some serious freezing within the fifth toe (far left). This makes physical sense as it is the smallest toe with the least volumetric heat generation through it. It would therefore be the least shielded from the cold and in reality, would see the worst effects. In contrast, we see the center of our foot having the warmest temperatures, as it is most shielded from the environment and typically would expect to see the least amount of freezing damage. Similarly, we see that under these conditions the center of the foot further towards the sole is largely unharmed after this time (Figure 3). A more mathematical depiction, showing the lower temperatures of the smaller outside toes, and the higher final temperatures of the big, pointer, and middle toes, is displayed in Figure 7. Given the volumetric heat generation through this region, it is physically reasonable that again we see the worst freezing around the skin, which would understandably freeze at this time while the center is left unharmed.

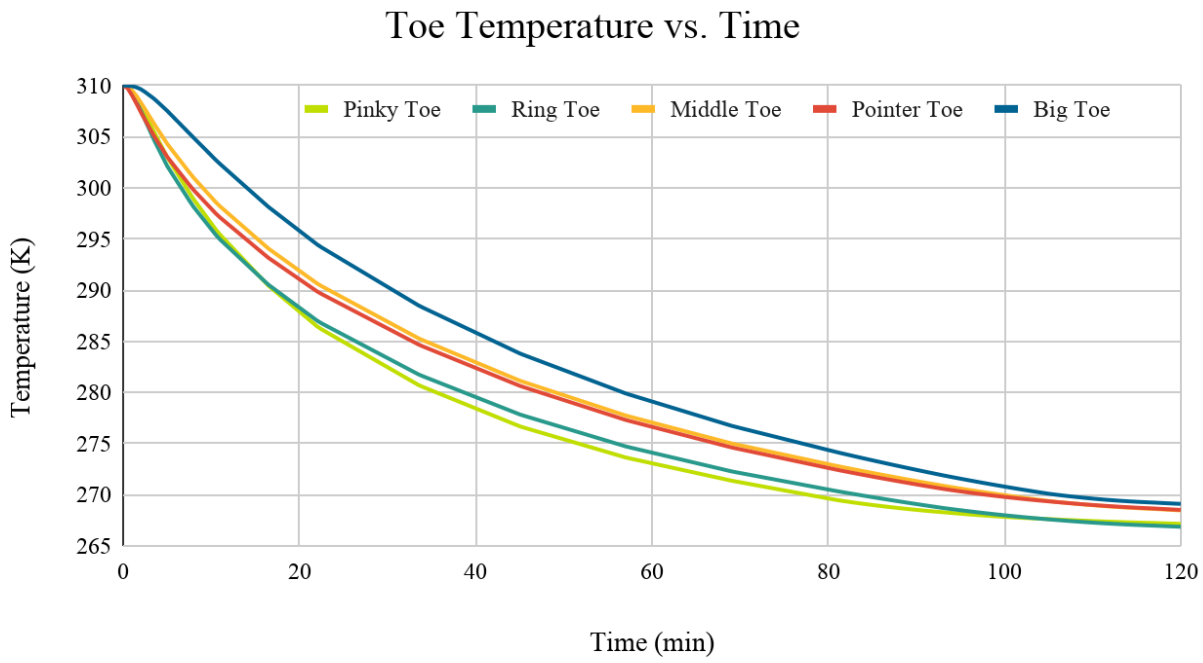

Figure 7: Temperature of five select representative points on in the toe region of the model as it changes over the course of the 120 minute run time. Coordinates for the points included can be found in Figure 5. Notice the difference in temperatures between the larger Big Toe and the smaller Pinky and Ring Toes, which can likely be attributed to an increase in metabolic heat generation. The inner two Pointer and Middle Toes arrive at a temperature between these extremes, likely due to their position in the middle of the geometry, shielding them from the harsh environment.

5.2 Reported Freezing Time of Exposed Tissue

As previously discussed, much of the available literature on the topic of frostbite is anecdotal. This yields minimal hard data that can be used for validation. Of the few concrete values, we found nearly all of them only had data relevant for *exposed* biological tissue. To compare against this we isolated the second toe from our full model (it was geometrically closest to a finger) and removed all insulation before subjecting it to freezing conditions. The isolated and exposed toe model began to experience subdermal freezing in 6 min. Experimental data from Wilson et al. showed freezing times of 8.4 +/- 2.8 min[16] of finger tissue under -15℃ and similar wind speeds. A finger simulation from Fallahi et al. predicted a time of 9.7 min to tissue freezing[1]. These values are all very close to our results and thus provide excellent validation that our model is on the right track and investigation of important parameters can begin.

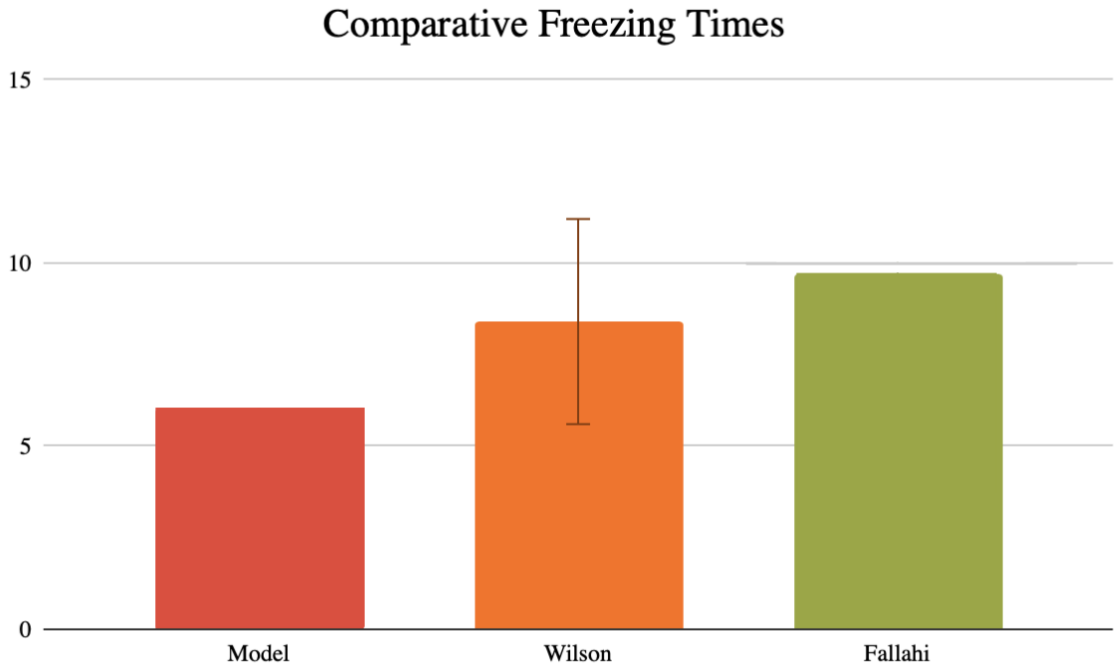

Fig. 8. Comparison of average initial freezing times for our model, experimental data (Wilson), and finger vasculature simulation(Fallaih). Here we see that our models freezing time is within the range specified in other studies.

5.3 Sensitivity Analysis

While it is wonderfully reassuring that many of our test values match up with previous literature, the goal of this work is not to provide quantitative analysis of the onset of frostbite. There are orders of magnitude potential variation in physical anatomical geometry, material properties, exposure conditions, and insulation conditions that are present in the real world. This means that while our model is accurate to its setup, the numerical values yielded (i.e. time to freeze) hold little predictive value to any other situation. While the model could be leveraged to simulate other conditions its real value is in establishing the most impactful parameters. For our sensitivity analysis, we tested four variables: metabolic heat generation rate, boundary condition heat transfer coefficient, thermal conductivity, and apparent specific heat. To compare the sensitivity of the model to each of these parameters in an equitable and meaningful way, we compared the baseline calculation to computations with a 10% increase and a 10% decrease in one of the variables at a time and compared the amount of frozen tissue in the model (Figure 9). The most significant variables are the specific heat and the thermal conductivity, which makes sense from a thermodynamics perspective. This also means that these values are the most crucial to get right in our final model.

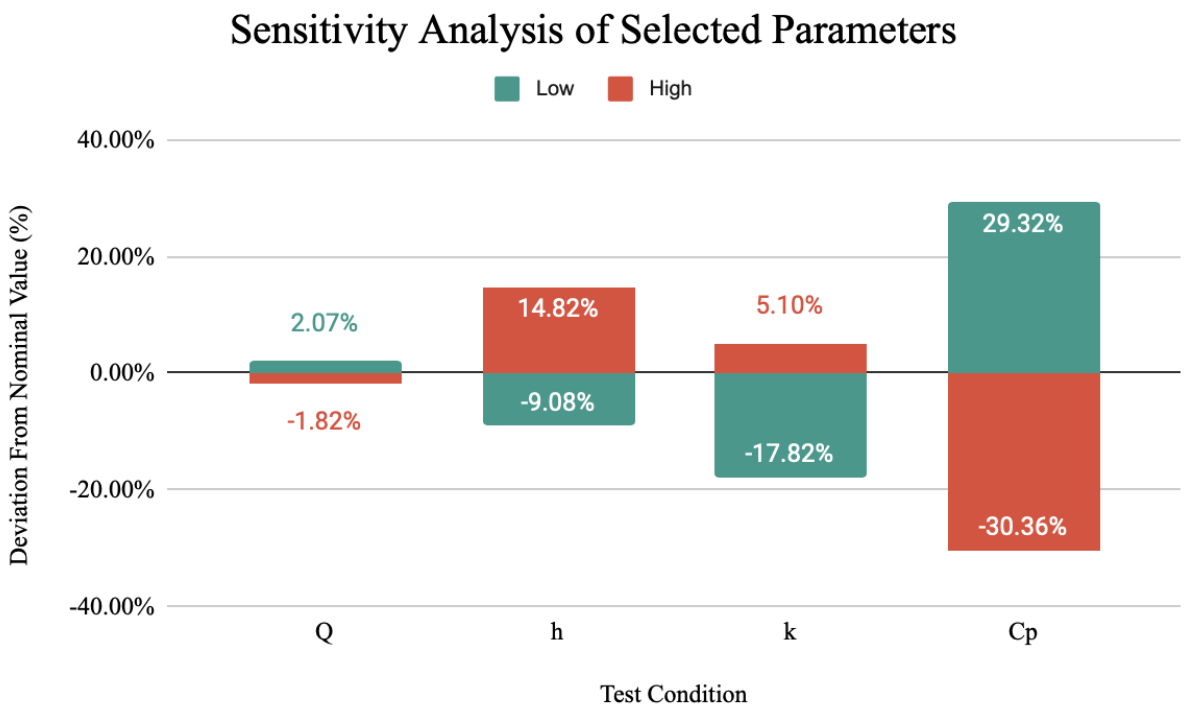

Figure 9: Sensitivity Analysis chart showing the change in amount of frozen tissue from the baseline computation. Values for thermal conductivity and metabolic heat generation can be found in Table 1. For apparent specific heat, only the values for -255°C, -25°C, -12°C, -2°C, 60°C were modified because the change in specific heat due to the latent heat of freezing of water is unlikely to change, so it did not make sense to modify these values (Table 2).

While these results may seem concrete, it is important to remember that the real-world feasibility of achieving a 10% deviation from nominal values may be drastically different for different parameters. For example, it may be much easier to effect an order of magnitude change in metabolic heat generation than to change thermal conductivity by a similar value. Further research and subsequent modeling are needed to ultimately determine the importance of each parameter with respect to their ease of modification.

6.0 Discussion of Realistic Constraints

6.1 Discussion of Future Applications

This design is purely for modeling purposes and should be used in the context of reducing the incidence of frostbite in future comparative studies. The significance and capability of this model reside entirely in heat transfer with potential freezing and should not be utilized outside of that realm. In research, the manipulation of select parameters within this model can yield positive results in developing novel solutions to frostbite.

The real significance of this design can then be implemented into a universe of real-world solutions that can adequately protect human appendages from any sort of inclement weather exposure. By manipulating any of the parameters in this anatomically accurate 3D model, researchers have the ability to quantitatively determine the proper insulative regime that can be used to adequately protect their subjects in whatever environment they choose.

When adjusting certain parameters in the context of this study, it will be important to consider which of the implemented parameters are reasonable to change to increase heat retention. For example, specific heat capacity is a fairly rigid function of material property, and ultimately cannot be changed as easily in future studies. However, any basis that this could change would require the adjustments of density and thermal conductivity associated with a novel material utilized.

6.2 Discussion of Health Safety, Ethical, and Economic Constraints

It will be important to remember that this model represents an average foot, and is not the perfect model for every individual's anatomy. Likely there will be key differences in proportions of toe to foot volume and fat content based on any one person. It must be noted that our model utilizes very specific environmental conditions that will not be representative of all regions and cold climates. Proper adjustments should be made from study to study.

From other studies, it is also clear that this model limits many concerns that would come up in experimentation regarding health safety and ethics. With frostbite being simultaneously very serious and treatable, little experimentation has or will be done on human patients. With this model, the dynamics of frostbite can be comfortably analyzed without the overarching concerns of subject harm.

In addition to the ethical advantages of our model, it also has economic value. The costs of real-world lab experiments which require freezing equipment and labor are far greater than the costs of running our model.

In summary, our model not only saves time, resources, and human test subjects but serves as a starting point for more accurate and efficient models. We hope that over time more researchers will be inspired by our model to create their own. This scaffold of data is necessary for all scientific research. Multitudes of trials and independent repetition of those trials are needed to gain an understanding of complex concepts. Our model serves as the initial replacement for experimentation that cannot be done ethically nor sustainably.

Our model is the first step for all future model-based frostbite research. Our toes have dipped into this unconventional, avant-garde geometric entanglement so that future researchers have the confidence and gusto to submerge their own feet into this mesh so that an accurate, authentic model can be converged upon by the scientific community and the hoi polloi.

7.0 References

[1] A. Fallahi, M. Reza Salimpour, and E. Shirani, "A 3D thermal model to analyze the temperature changes of digits during cold stress and predict the danger of frostbite in human fingers," *Journal of Thermal Biology*, vol. 65, pp. 153–160, Apr. 2017, doi: 10.1016/j.jtherbio.2017.03.001.

[2] V. Vuksanović, L. W. Sheppard, and A. Stefanovska, "Nonlinear Relationship between Level of Blood Flow and Skin Temperature for Different Dynamics of Temperature Change," *Biophys J*, vol. 94, no. 10, pp. L78–L80, May 2008, doi: 10.1529/biophysj.107.127860.

[3] M. A. Hashmi, M. Rashid, A. Haleem, S. A. Bokhari, and T. Hussain, "Frostbite: epidemiology at high altitude in the Karakoram mountains.," *Ann R Coll Surg Engl*, vol. 80, no. 2, pp. 91–95, Mar. 1998.

[4] D. S. Martin, C. Ince, P. Goedhart, D. Z. H. Levett, M. P. W. Grocott, and for the Caudwell Xtreme Everest Research Group, "Abnormal blood flow in the sublingual microcirculation at high altitude," *Eur J Appl Physiol*, vol. 106, no. 3, pp. 473–478, Jun. 2009, doi: 10.1007/s00421-009-1023-8.

[5] D. I. Lawson, P. H. Thomas, and D. L. Simms, "THE THERMAL PROPERTIES OF SKIN," *Fire Safety Science*, vol. 224, 1955. Available: https://www.iafss.org/publications/frn/224/-1.

[6] Y. Lee and K. Hwang, "Skin thickness of Korean adults," Surg Radiol Anat, vol. 24, no. 3, pp. 183–189, Jan. 2002, doi: 10.1007/s00276-002-0034-5.

[7] "Thermal Conductivity » IT'IS Foundation." https://itis.swiss/virtual-population/tissue-properties/database/thermal-conductivity/.

[8] 'Frostbite and Hypothermia.' American Burn Association, www.ameriburn.org.

[9] "Specific Heat Capacities of Air - (Updated 7/26/08)." https://www.ohio.edu/mechanical/thermo/property_tables/air/air_Cp_Cv.html.

[11] "Thermal Conductivity of some Selected Materials and Gases." https://www.engineeringtoolbox.com/thermal-conductivity-d_429.html

[12] “Density of Selected Solids.” https://www.engineeringtoolbox.com/density-solids-d_1265.html.

[13] “Specific Heat of Solids.” https://www.engineeringtoolbox.com/specific-heat-solids-d_154.html.

[14] “THERMAL PROPERTIES OF FOOD.” *TNTech*, Computer-Aided Engineering Network, www.cae.tntech.edu/~jbiernacki/CHE%204410%202016/Thermal%20Properties%20of%20Foods.pdf.

[15] M. D. Andrews, “Cryosurgery for Common Skin Conditions,” *AFP*, vol. 69, no. 10, pp. 2365–2372, May 2004. https://www.aafp.org/afp/2004/0515/p2365.html

[16] O. Wilson, R. F. Goldman, and G. W. Molnar, “Freezing temperature of finger skin,” *Journal of Applied Physiology*, vol. 41, no. 4, pp. 551–558, Oct. 1976, doi: 10.1152/jappl.1976.41.4.551.

[17] Thingiverse.com, “Anatomic Human Foot & Lower Extremity Version 2.0 by DrGlassDPM.” https://www.thingiverse.com/thing:22628 (accessed Apr. 16, 2021).

[18] C. K. Holland, J. M. Brown, L. M. Scoutt, and K. J. W. Taylor, “Lower extremity volumetric arterial blood flow in normal subjects,” *Ultrasound in Medicine & Biology*, vol. 24, no. 8, pp. 1079–1086, Oct. 1998, doi: 10.1016/S0301-5629(98)00103-3.

[19] J. Grayson, “Cold and Warmth Vasoconstriction Responses in the Skin of Man,” [Online]. Available: https://heart.bmj.com/content/heartjnl/13/2/167.full.pdf.

8.0 Appendices

8.1 Appendix A

	Skin	**Flesh**	**Subcutaneous Fat**	**Sock**	**Air**	**Boot**
Thermal Conductivity (W/mK)	0.37[5]	0.49[7]	0.21[7]	0.04[11]	1.4[9]	0.14[11]
Density (kg/m^3)	1109[5]	1090[12]	911[12]	1314[12]	1.2466[9]	860[12]
Freezing Point (℃)	0[16]	0	0	N/A	N/A	N/A
Heat Generation Rate (W/kg)	1.65[5]	0.91[5]	0.51[5]	0	0	0

Table 1. Necessary thermodynamic values for the various layers in the model. Specific Heat is specified before and after freezing as changing internal temperature will change this as it solidifies. We assume here that sock and boot layers are both entirely dry and generate no heat.

Temp (K)	18	248	261	265	265	269	270	270.5	271	333
$C_{p,a}$ (J/K)	4180	4180	5000	10000	20000	80000	44000	20000	4180	4180

Table 2. Parametrized apparent specific heat values used in all tissue layers. These values replace the static specific heats used previously in favor of a dynamic apparent specific heat that takes into account the latent heat needed to freeze the water in the tissue around 0°C.

8.2 Appendix B

```
Time-stepping completed.
Solution time: 6974 s. (1 hour, 56 minutes, 14 seconds)
Physical memory: 12.79 GB
Virtual memory: 21.37 GB
```

Figure 10: Screenshot of a normal COMSOL computation run. Detailed are the memory and time requirements for a standard run of the model.